Linear and Nonlinear Optical Characteristics of the Falicov-Kimball Model

T. Portengen, Th. Östreich, and L. J. Sham
Department of Physics, University of California San Diego, La Jolla, California 92093-0319
(Received 20 July 1995)

We calculate the linear and nonlinear optical properties of the Falicov-Kimball model for a mixed-valent system within the self-consistent mean-field approximation. Second-harmonic generation can only occur if the mixed-valent state has a built-in coherence between the itinerant d electrons and the localized f holes. By contrast, second-harmonic generation cannot occur for solutions of the model with f-site occupation as a good quantum number. As an experimental test of coherence in mixed-valent compounds we propose a measurement of the dynamic second-order susceptibility. [S0031-9007(96)00021-X]

PACS numbers: 71.28.+d, 42.65.Ky, 78.20.Ci

The Falicov-Kimball (FK) [1] model has been used extensively for the mixed-valent compounds, heavy fermion systems, and associated metal-insulator transitions. The FK model accounts for a band of itinerant d electrons and localized f orbitals and intrasite Coulomb interaction between the d and f electrons. A d-f hybridization term may or may not be added to the model. The theoretical solutions for the ground state of the FK model can be divided into two classes. On the one hand, solutions that treat the occupation of an f electron on a site as a good quantum number [2,3] do not have a built-in coherence between d electrons and f holes. On the other hand, solutions such as the self-consistent mean-field solution [4] and the electronic polaron [5] do have a built-in coherence between d electrons and f holes.

We report here the nonlinear optical responses of these two classes of solutions. Solutions of the model with a built-in coherence can sustain second-harmonic generation. Solutions with classical f-electron site distributions cannot. Therefore, we propose the measurement of the second-order susceptibility of a mixed-valent compound as a test to distinguish between these theories. The existence of such second-harmonic generation due to coherence in the ground state would, of course, be of interest in its own right as a manifestation of strong electron correlation.

Four-wave-mixing (FWM) spectroscopy has become a powerful tool for studying coherence in semiconductor systems [6]. In a three-beam FWM experiment, two incoming beams of wave vectors $\mathbf{k}_1$ and $\mathbf{k}_2$ set up a transient polarization grating. The third incoming beam of wave vector $\mathbf{k}_3$ diffracts off the grating to produce the outgoing signal in the direction $\mathbf{k}_4 = \mathbf{k}_3 + \mathbf{k}_2 - \mathbf{k}_1$. Being a third-order process, FWM is allowed in media with or without inversion symmetry. We pose the question: What happens if the state being probed already has a polarization built into it instead of being created artificially by optical pumping? An example of such a system is the self-consistent mean-field (SCMF) solution of the FK model resulting in the Bose-Einstein condensation of d-f excitons.

As shown below, the built-in polarization leads to a nonlinear optical response to *second* order in the external field. The built-in polarization replaces one of the external fields of the three-beam FWM experiment. The mixed-valent system has a nonvanishing susceptibility $\chi^{(2)}(2\omega, \omega, \omega)$ for second-harmonic generation. In crystals with inversion symmetry, second-harmonic generation is forbidden under the electric-dipole approximation. In the mixed-valent system, the built-in polarization breaks the inversion symmetry, allowing second-harmonic generation to take place. The built-in polarization also means that the system is ferroelectric. Our calculation of the concomitant dielectric behavior will be reported elsewhere. There are reports of unusually large dielectric constants in mixed-valent semiconductors [7]. Because of the problem of residual carriers in dielectric measurements, we feel that the nonlinear optical effect might be a clearer test.

We present a calculation of the linear and second-harmonic susceptibilities of a model mixed-valent system within the SCMF approximation. The magnitude of the second-harmonic output signal is directly proportional to the built-in coherence Δ. The Coulomb interaction between the optically excited quasiparticles greatly enhances the second-harmonic conversion efficiency at $\omega = \Delta$ (one half the energy gap 2Δ).

Ignoring the electron spin, the FK Hamiltonian is

$$H = \sum_{\mathbf{k}} \varepsilon_{\mathbf{k}} d_{\mathbf{k}}^{\dagger} d_{\mathbf{k}} + E_f' \sum_{\mathbf{k}} f_{\mathbf{k}}^{\dagger} f_{\mathbf{k}} + \sum_{\mathbf{k}} (V_{\mathbf{k}} d_{\mathbf{k}}^{\dagger} f_{\mathbf{k}} + \text{H.c.}) + \frac{U}{N} \sum_{\mathbf{k},\mathbf{k}',\mathbf{q}} d_{\mathbf{k}+\mathbf{q}}^{\dagger} d_{\mathbf{k}} f_{\mathbf{k}'-\mathbf{q}}^{\dagger} f_{\mathbf{k}'} . \quad (1)$$

Here $d_{\mathbf{k}}^{\dagger}$ ($f_{\mathbf{k}}^{\dagger}$) creates a d (f) electron of momentum $\mathbf{k}$ and energy $\varepsilon_{\mathbf{k}}$ (E_f'). The parameters U and $V_{\mathbf{k}}$ are the direct interaction and the hybridization between the d and f electrons, and N is the number of sites. We consider a model system with a d band and f level arising from d and f orbitals on the same site. The d band has bandwidth $2W$ and a constant density of states $\rho_0 = 1/(2W)$.

The SCMF solution is analogous to the BCS theory of superconductivity except that the pairing now occurs between a d electron of momentum $\mathbf{k}$ and an f hole of momentum $-\mathbf{k}$. The ground state is $|\psi\rangle = \prod_{\mathbf{k}} (u_{\mathbf{k}} +$

 0031-9007/96/76(18)/3384(4)$10.00

$v_{\mathbf{k}} d_{\mathbf{k}}^{\dagger} f_{\mathbf{k}}) |0\rangle$, where $|0\rangle$ is the state with no f holes (the normal state), and $v_{\mathbf{k}}$ ($u_{\mathbf{k}}$) is the probability amplitude for the pair state $(\mathbf{k}, -\mathbf{k})$ to be occupied (unoccupied).

A key feature of $|\psi\rangle$ is that it is a state of broken inversion symmetry. If the crystal is invariant under inversion with respect to a d-f site, the inversion symmetry is broken by the pairing of d states of even parity with f states of odd parity. Applying the inversion $\hat{J}$ on $|\psi\rangle$ yields the state $\hat{J}|\psi\rangle = \prod_{\mathbf{k}} (u_{\mathbf{k}}^{*} - v_{\mathbf{k}}^{*} d_{\mathbf{k}}^{\dagger} f_{\mathbf{k}}) |0\rangle$, which is orthogonal to $|\psi\rangle$ and has the same energy except in the case $U = 0$ when the two states are the same. The degenerate states $|\psi\rangle$ and $\hat{J}|\psi\rangle$ have built-in polarizations of opposite directions, for the polarization operator $\hat{\mathbf{P}} = (\sum_{\mathbf{k}} \mu d_{\mathbf{k}}^{\dagger} f_{\mathbf{k}} + \text{H.c.})/\Omega$ where Ω is the system volume. We take the interband dipole matrix element μ to be independent of $\mathbf{k}$. The correct ground state is selected by lifting the degeneracy with an infinitesimal external electric field $\mathbf{E}$, and choosing the lower energy state. The consequent breaking of the inversion symmetry is what allows second-harmonic generation to take place.

The built-in polarization defines a direction in space, which we call the z axis. (Without crystal-field terms, the z axis has no definite orientation with respect to the crystal axes.) Since μ_z is real, $P_z^{(0)} = N\mu_z(\Delta + \Delta^{*})/\Omega U$, where Δ is the built-in coherence. The built-in coherence is determined self-consistently from

$$\Delta = \frac{U}{N} \sum_{\mathbf{k}} \frac{\Delta - V_{\mathbf{k}}}{2E_{\mathbf{k}}}, \tag{2}$$

where $2E_{\mathbf{k}} = \sqrt{(\varepsilon_{\mathbf{k}} - E_f)^2 + 4|\Delta - V_{\mathbf{k}}|^2}$ is the quasielectron-hole pair excitation energy [8]. Equation (2) is Eq. (11) of Ref. [4] with a $\mathbf{k}$-dependent hybridization. If the crystal is invariant under inversion, the hybridization must satisfy $V_{-\mathbf{k}} = -V_{\mathbf{k}}$. Then, since $V_{\mathbf{k}}$ is purely imaginary and odd in $\mathbf{k}$, the imaginary part of Δ vanishes due to the cancellation of terms with $\pm\mathbf{k}$. The real part of Δ is given by the BCS gap equation

$$\Delta = \frac{U}{N} \sum_{\mathbf{k}} \frac{\Delta}{2E_{\mathbf{k}}}, \tag{3}$$

with $2E_{\mathbf{k}} = \sqrt{(\varepsilon_{\mathbf{k}} - E_f)^2 + 4\Delta^2 + 4|V_{\mathbf{k}}|^2}$. Calculation shows that sufficiently strong $V_{\mathbf{k}}$ can destroy the gap. In the following we consider the limit where $V_{\mathbf{k}}$ is negligible.

Δ is the order parameter of the valence transition. When the f level is far below the d band, the system is in the normal state ($\Delta = 0$). As the f level is moved upward past a critical value (in a real material this is done by applying pressure or alloying), the system undergoes a transition into the mixed-valent state ($\Delta > 0$). In the mixed-valent state, the f-level occupancy n_f lies between 0 and 1. Δ reaches a maximum at the half-filling point $E_f = 0$. Electron-hole symmetry requires $\Delta(-E_f) = \Delta(E_f)$ and $n_f(-E_f) = 1 - n_f(E_f)$.

We first consider the linear absorption spectrum of the mixed-valent system. The SCMF solution predicts an energy gap 2Δ. Far-infrared optical measurements [9–11], as well as electron tunneling experiments [12], show an energy gap of several meV in a number of mixed-valent compounds. The crucial difference between the superconductor and the mixed-valent system is this: in the superconductor, the pairing occurs between two *electrons*, whereas in the mixed-valent system, the pairing occurs between an *electron* and a *hole*. This has important consequences for the coherence factors that enter the response of both systems to different external probes. For example, the coherence factor entering the *optical* absorption of the mixed-valent system is the same as the coherence factor entering the *acoustic* attenuation of the superconductor. The interaction of the mixed-valent system with the electromagnetic field is treated in the electric-dipole approximation. Only the component of the electric field along the symmetry-breaking z axis couples to the channel in which the pairing takes place. We ignore the response of the remaining optical channels. Second-harmonic generation can only occur in the symmetry-breaking channel.

We have calculated the linear susceptibility $\chi_{zz}^{(1)}$ both from the Kubo formula and from the optical Bloch equations. The pseudospin picture gives a nice physical description of the linear and nonlinear responses as precessional modes of the pseudospin $\mathbf{S}_{\mathbf{k}}$. For a given $\mathbf{k}$, the pseudospin corresponds to the $d_{\mathbf{k}}$ and the $f_{\mathbf{k}}$ states as a two-level system. The equations of motion for the pseudospin are the optical Bloch equations

$$\dot{\mathbf{S}}_{\mathbf{k}} = (\mathbf{H}_{\mathbf{k}} - \mathbf{M}_{\mathbf{k}}) \times \mathbf{S}_{\mathbf{k}}. \tag{4}$$

Here $\mathbf{H}_{\mathbf{k}} = (-2\mu_z E_z, 0, \varepsilon_{\mathbf{k}} - E_f')$ is the external "magnetic" field, and $\mathbf{M}_{\mathbf{k}} = (U/N)\sum_{\mathbf{k}} \mathbf{S}_{\mathbf{k}}$ is the pseudomagnetization. The symbol $\times$ means the vector cross product.

To calculate the linear susceptibility we expand $\mathbf{S}_{\mathbf{k}}$, $\mathbf{H}_{\mathbf{k}}$, and $\mathbf{M}_{\mathbf{k}}$ to first order in the electric field E_z. From Eq. (4) to zeroth order we obtain an equation for the stationary pseudospin $\mathbf{S}_{\mathbf{k}}^{(0)}$. The built-in coherence tilts $\mathbf{S}_{\mathbf{k}}^{(0)}$ away from the negative z axis. The tilting angle is $\theta_{\mathbf{k}} = \arccos(v_{\mathbf{k}}^2 - u_{\mathbf{k}}^2)$. For Δ real, $\mathbf{S}_{\mathbf{k}}^{(0)}$ lies in the x-z plane. The electric field causes the pseudospin to precess around the stationary direction. With the precession axis tilted away from the z axis, the field causes variations in all three Cartesian components of $\mathbf{S}_{\mathbf{k}}$. A simpler description is obtained in the spherical polar coordinate system. The stationary direction is the radial unit vector $\mathbf{e}_r$. The precession is decomposed into components along the polar and azimuthal unit vectors $\mathbf{e}_{\theta}$ and $\mathbf{e}_{\phi}$. The equations of motion for the polar and azimuthal components $S_{\theta,\mathbf{k}}^{(1)}$ and $S_{\phi,\mathbf{k}}^{(1)}$ are

$$\dot{S}_{\theta,\mathbf{k}}^{(1)} - 2E_{\mathbf{k}} S_{\phi,\mathbf{k}}^{(1)} + M_{\phi,\mathbf{k}}^{(1)} = F_{\theta,\mathbf{k}}^{(1)}, \tag{5}$$

$$\dot{S}_{\phi,\mathbf{k}}^{(1)} + 2E_{\mathbf{k}} S_{\theta,\mathbf{k}}^{(1)} - M_{\theta,\mathbf{k}}^{(1)} = F_{\phi,\mathbf{k}}^{(1)}. \tag{6}$$

The driving terms are $F_{\theta,\mathbf{k}}^{(1)} = 0$ and $F_{\phi,\mathbf{k}}^{(1)} = 2\mu_z E_z \cos\theta_{\mathbf{k}}$. The linear susceptibility is $\chi_{zz}^{(1)} = P_z^{(1)}/E_z$, where $P_z^{(1)} = (N\mu_z \sum_{\mathbf{k}} S_{\theta,\mathbf{k}}^{(1)} \cos\theta_{\mathbf{k}})/\Omega$ is the linear polarization.

For a separable interaction potential, Eqs. (5) and (6) can be solved analytically. The linear susceptibility is

$$\chi^{(1)}_{zz} = \frac{2N\mu_z^2}{\Omega U}\left(\frac{A(\omega)}{(\omega^2 - 4\Delta^2)A^2(\omega) - B^2(\omega)} - 1\right), \tag{7}$$

where

$$A(\omega) = \frac{U}{N}\sum_{\mathbf{k}} \frac{1}{2E_{\mathbf{k}}(\omega - 2E_{\mathbf{k}})(\omega + 2E_{\mathbf{k}})}, \tag{8}$$

$$B(\omega) = \frac{U}{N}\sum_{\mathbf{k}} \frac{\varepsilon_{\mathbf{k}} - E_f}{2E_{\mathbf{k}}(\omega - 2E_{\mathbf{k}})(\omega + 2E_{\mathbf{k}})}. \tag{9}$$

For the simple model system, $A(\omega)$ and $B(\omega)$ can be expressed in terms of elementary functions. The poles of $\chi^{(1)}_{zz}$ give the collective excitation energies of the mixed-valent system. The denominator in Eq. (7) vanishes when $(\omega^2 - 4\Delta^2)A^2(\omega) - B^2(\omega) = 0$. The zero-frequency Goldstone mode is a consequence of the arbitrariness of the phase of Δ (in the absence of hybridization). In the pseudospin picture, the Goldstone mode corresponds to rotating all pseudospins around the z axis over the same angle ϕ. Since this does not change the total energy, the Goldstone mode has zero frequency. In Eq. (7), the Goldstone mode does not appear to contribute to the linear optical response since the pole at $\omega = 0$ is canceled by a factor of ω in the numerator. There are no excitonlike collective modes within the energy gap. When $\omega < 2\Delta$, the functions $A(\omega)$ and $B(\omega)$ are purely real, so $(\omega^2 - 4\Delta^2)A^2(\omega) - B^2(\omega) < 0$.

The absorption spectrum is given by the imaginary part of $\chi^{(1)}_{zz}$. When the f level lies inside the d band ($|E_f| \leq W$), the absorption spectrum has a threshold singularity at $\omega = 2\Delta$. When $|E_f| < W$, the singularity is $\epsilon^{-1/2}\theta(\epsilon)$, and when $|E_f| = W$ the singularity is $\epsilon^{-1/2}\ln^{-2}(\epsilon)\theta(\epsilon)$, where $\epsilon = \omega - 2\Delta$. When the f level lies outside the d band, the singularity is cut off because the energy gap is larger than 2Δ. The singularity is due to the final-state Coulomb interaction between the optically excited quasiparticles. In the single-quasiparticle picture, the absorption spectrum rises continuously from zero according to $\epsilon^{1/2}\theta(\epsilon)$. The singularity is *not* an artifact of the simple model, and should be observable in real materials.

We calculate the second-harmonic susceptibility $\chi^{(2)}_{zzz}$ from the optical Bloch equations by expanding the pseudospin and the pseudomagnetization to *second* order in the perturbing electric field E_z. The equations of motion for the second-order components $S^{(2)}_{\theta,\mathbf{k}}$ and $S^{(2)}_{\phi,\mathbf{k}}$ have the same form as Eqs. (5) and (6), except with more complicated driving terms. A very important observation is that all driving terms are directly proportional to Δ. When $\Delta = 0$, the second-harmonic susceptibility vanishes identically.

In addition, the second order fluctuations have a nonzero radial component $S^{(2)}_{r,\mathbf{k}}$. The motion is no longer a regular precession: the pseudospin *nutates* during the precession. (Nutation is the up-and-down motion of the precession axis.) The nutation frequency is twice the precession frequency. The second-harmonic susceptibility is $\chi^{(2)}_{zzz} = P^{(2)}_z/E^2_z$, where $P^{(2)}_z = [N\mu_z\sum_{\mathbf{k}}(S^{(2)}_{\theta,\mathbf{k}}\cos\theta_{\mathbf{k}} + S^{(2)}_{r,\mathbf{k}} \times \sin\theta_{\mathbf{k}})]/\Omega$ is the second-order polarization.

For a separable interaction potential, an analytic solution for the second-harmonic response is possible in principle. However, the large number of driving terms presents a considerable challenge. We have instead approached the problem numerically. This is done in analogy with the classical mechanics treatment of forced oscillations. One first solves for the motion in normal coordinates, and then takes linear combinations to obtain the motion in the original coordinates. The results of the calculation are shown in Fig. 1. The figure shows the amplitude $|\chi^{(2)}_{zzz}(2\omega,\omega,\omega)|$ of the second-harmonic susceptibility as a function of the photon energy ω, for various values of E_f. The important features are the following: (1) The second-harmonic amplitude is directly proportional to the amount of coherence Δ built into the mixed-valent system. (2) When the f level lies inside the d band, the second-harmonic conversion efficiency is strongly enhanced at $\omega = \Delta$, and less strongly at $\omega = 2\Delta$. The first feature shows that second-harmonic generation can be used as a test of the validity of the SCMF solution in real mixed-valent materials. The second feature distinguishes the single-quasiparticle treatment of the second-harmonic response from the self-consistent mean-field treatment. Like the threshold singularity in the case of linear response, the enhancement of the second-harmonic conversion efficiency is due to the final-state Coulomb interaction between the optically excited quasiparticles.

As an experimental test of coherence in mixed-valent compounds we propose a measurement of their second-harmonic susceptibility $\chi^{(2)}(2\omega,\omega,\omega)$. Consider, for

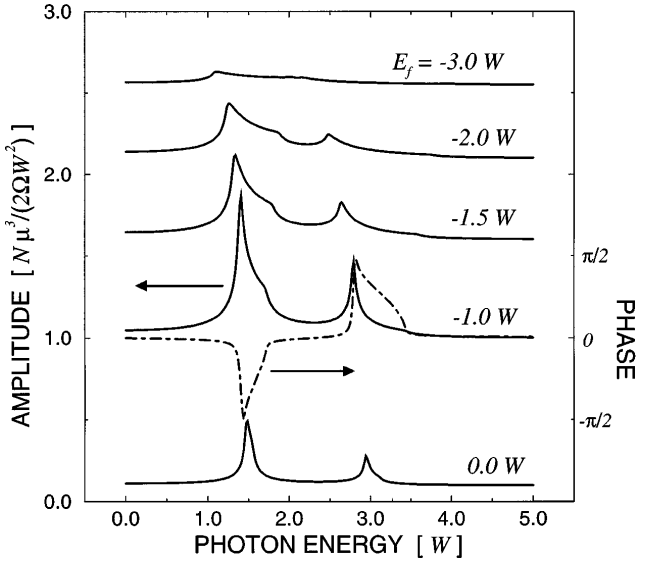

FIG. 1. Amplitude $|\chi^{(2)}_{zzz}(2\omega,\omega,\omega)|$ of the second-harmonic susceptibility as a function of the photon energy ω, for various values of the f level E_f. The dash-dotted line shows the phase of $\chi^{(2)}_{zzz}(2\omega,\omega,\omega)$ for $E_f = -1.0W$. The Coulomb repulsion is $U = 3.0W$, and the hybridization is $V_{\mathbf{k}} = 0$. The amplitude is given in units of $N\mu_z^3/2\Omega W^2$. For the parameter values given for the solid line in Fig. 2, $N\mu_z^3/2\Omega W^2 = 82\ \mathrm{nm\,V^{-1}}$.

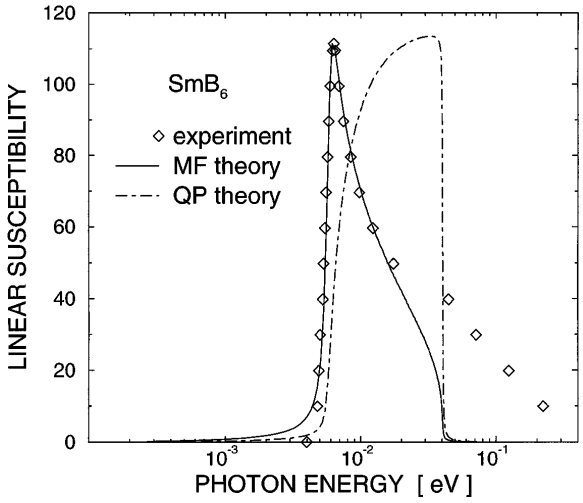

FIG. 2. Comparison of the mean-field (solid line) and single-quasiparticle (dash-dotted line) results for the imaginary part of the linear susceptibility $\chi^{(1)}_{zz}(\omega)$ of SmB_6 to experimental data taken from Ref. [10] (diamonds). The f level is $E_f = 0$, the bandwidth is $W = 40$ meV, the Coulomb repulsion is $U = 0.38W$, and the hybridization is $V_{\mathbf{k}} = 0$. The photon energy ω was given a small imaginary part $\delta = 0.01W$. The interband dipole matrix element is $\mu_z = 4.4ea_0$ for the solid line, and $\mu_z = 5.0ea_0$ for the dash-dotted line.

example, SmB_6. The crystal structure of SmB_6 has cubic symmetry, with B_6 octahedra at the body center, and Sm ions at the corners of a conventional bcc unit cell with lattice constant $a = 4.13$ Å. The crystal has inversion symmetry at the bcc lattice points. Through measurements of the ionic radius, the valence of the Sm ion in SmB_6 is found to be 2.53, almost halfway between 2 and 3, so that the f level lies near the center of the conduction band. The measured far-infrared absorption spectrum [9–11] of SmB_6 can be interpreted in accordance with the SCMF solution. In Fig. 2 we compare the mean-field and single-quasiparticle results for the linear susceptibility to experimental data on SmB_6 taken from Ref. [9]. The data show an energy gap around $2\Delta = 4$ meV, and a sharp peak at threshold. The mean-field theory fits the data very well in the threshold region, whereas the single-quasiparticle theory gives a qualitatively wrong threshold behavior. Away from threshold, discrepancies between mean-field theory and experiment occur because of our simple model density of states. Further experimental indication for the validity of the SCMF solution in SmB_6 is provided by the electron tunneling spectrum [12], which can be explained by analogy with Giaever tunneling in superconductors.

The second-harmonic generation for the other types of solutions of the FK model is now discussed briefly. If the f occupancy at each site is a good quantum number (0 or 1), any solution [2,3], homogeneous or inhomogeneous, will not give rise to second-harmonic generation. For the electronic polaron solution [5], the nonzero coherence yields a second-harmonic generation. We found $\Delta = 3.28W$ for the parameter values given in Ref. [5]. To distinguish between the exciton condensation solution and the electronic polaron requires an investigation of the quantitative difference of their linear and nonlinear optical spectra. Such a theoretical study will be left for the future.

In conclusion, we calculated the linear and nonlinear optical characteristics of the Falicov-Kimball model within the SCMF approximation. We found that the second-harmonic susceptibility is directly proportional to the amount of coherence Δ built into the mixed-valent system. We also found that the final-state Coulomb interaction leads to a threshold singularity in the absorption spectrum, and strongly enhances the second-harmonic conversion efficiency at $\omega = \Delta$. As an experimental test of the validity of the SCMF solution in real mixed-valent materials we propose a measurement of $\chi^{(2)}(2\omega, \omega, \omega)$.

L. J. S. wishes to thank Dr. M. B. Maple and Dr. S. H. Liu for stimulating conversations. This work was supported in part by NSF Grant No. DMR 94-21966 and in part by the Deutsche Forschungsgemeinschaft (DFG).

[1] L. M. Falicov and J. C. Kimball, Phys. Rev. Lett. **22**, 997 (1969); R. Ramirez, L. M. Falicov, and J. C. Kimball, Phys. Rev. B **2**, 3383 (1970).
[2] J. K. Freericks and L. M. Falicov, Phys. Rev. B **41**, 2163 (1990).
[3] For a review of recent papers on the FK model, see P. Farkašovský, Phys. Rev. B **51**, 1507 (1995).
[4] H. J. Leder, Solid State Commun. **27**, 579 (1978).
[5] S. H. Liu, Phys. Rev. B **37**, 3542 (1988).
[6] D. S. Kim *et al.*, Phys. Rev. Lett. **69**, 2725 (1992).
[7] H. Goto *et al.*, J. Phys. Soc. Jpn. **62**, 1365 (1993).
[8] We shall use the renormalized f level $E_f = E'_f + U(1 - 2n_f)$ as the materials parameter.
[9] P. Wachter and G. Travaglini, J. Magn. Magn. Mater. **47–48**, 423 (1985).
[10] S. von Molnar *et al.*, in *Valence Instabilities*, edited by P. Wachter and H. Boppart (North-Holland, Amsterdam, 1982).
[11] B. Batlogg, P. H. Schmidt, and J. M. Rowell, in *Valence Fluctuations in Solids*, edited by L. M. Falicov, W. Hanke, and M. B. Maple (North-Holland, Amsterdam, 1981).
[12] G. Güntherodt, W. A. Thompson, F. Holtzberg, and Z. Fisk, in *Valence Instabilities* (Ref. [10]).